Colloid & Polymer Science Colloid Polym Sci 272:1–16 (1994)

Original contributions

The isothermal crystallization of engineering polymers – POM and PEEK*)

J. J. C. Cruz-Pinto, J. A. Martins and M. J. Oliveira

Department of Polymer Engineering, Universidade do Minho, Braga, Portugal

Abstract: The isothermal crystallization of two engineering polymers – POM and PEEK – was studied, both theoretically and experimentally. The experiments were performed by means of differential scanning calorimetry (DSC) and polarized light optical microscopy (OM).

Building on previously developed theoretical formalisms (Avrami/Evans, Hillier and Tobin), a new procedure is presented, based on Tobin's model coupled with a modification of Hillier's calculation technique, to accurately describe the kinetics and mechanism of the crystallization of polymers from quiescent melts. First, it is shown that Tobin's model alone, without modification, is more accurate than Avrami/Evans model to describe single-mechanism processes, for a wide range of materials and for longer crystallization times, despite having exactly the same nature and number of parameters (the kinetic, nucleation and growth rate-related, parameter K and the dimensionality n). Then, Hillier's formalism is modified and combined with Tobin's model, to accurately predict the kinetics of dual mechanism crystallization processes; a clear contrast is drawn with Hillier's Avrami-based, original procedure which uses the same number and nature of parameters, but cannot adequately predict the experimental behavior.

The parameter values predicted by the model(s) and procedure presented in this work are all given, are then physically interpreted and, in the case of POM, related to independent morphological observations by polarized light optical microscopy. They are also consistent with electron microscopy observations made by other authors on the detailed morphology of the spherulitic crystallization of polymers.

Key words: Polymer crystallization – kinetics – modeling – POM – PEEK

1. Introduction

Despite all pioneering and more recent contributions to the subject, the kinetics of polymer crystallization still lacks a clear and accurate quantitative description; even simple, single-mechanism crystallization processes still defy truly accurate modeling from first principles and basic experimental data.

Previous and recent works almost exclusively adopted the early analyses developed by Avrami [1–3] and Evans [4], overlooking many of their well established limitations [5], and unfairly neglecting the work published by Tobin [6–8], which provided a significantly different model of the overall crystallization kinetics. The somewhat superficial physical discussion of the model in Tobin's papers may have contributed to their relative neglect, but the fact remains that, despite the widespread use and acceptance of Avrami/Evans analyses, their accuracy is very poor, and the resulting kinetic parameters values are often difficult to understand and justify [5, 9].

*) Presented at the EPS-Meeting "Solidification Processes in Polymers" in Stockholm May 1991

In addition to Tobin's model, which will be discussed and justified in this work (and may also be generalized [10]), the other most significant contribution to the modeling of the overall kinetics of polymer crystallization is due to Hillier [11]. Although the basis still is an Avrami-like description of single-mechanism processes, Hillier's work brought a real advance by clearly pointing out how different sequential and/or simultaneous mechanisms may contribute to, and be combined in, complex crystallization processes.

Other more recent attempts based on simple parallel or serial combinations of integrated Avrami equations [12, 13] are difficult to physically justify [9], and will not be discussed here, Reference [9] details how two or more strictly serial or parallel mechanisms may be accurately combined in the same overall complex process, but Hillier's type of approach, being of greater generality, is favored here.

In this work, the crystallization of a poly(oxymethylene) – POM – and of a poly(ether-ether-ketone) – PEEK – are studied both theoretically and experimentally (mainly by means of dual-furnace, power-compensated, DSC measurements, and also by optical microscopy observations) to accurately characterize and model the kinetics of simple and complex polymer crystallization processes. The generality of the models and methods is highlighted, as they are useful for a wide range of materials, e.g. polymers and metals.

2. Modeling of single-mechanism crystallization processes

2.1. Avrami/Evans model

The analyses due to Avrami [1–3] and Evans [4] are well known and even documented in textbooks [14, 15].

Briefly, for a given geometry of growth and type of nucleation (instantaneous or sporadic), the mass fraction of material that crystallizes up to time t, assuming no interaction with neighboring crystalline material (free growth approximation), may be shown to be, at least approximately, $X' = Kt^n$, with $n = 3$ or 4 for spherulitic crystallization with instantaneous or sporadic nucleation, respectively. Then, the true fraction of crystallized material, allowing for interaction and impingement of neighboring growing spherulites, is obtained as $X = 1 - \exp(-X')$.

The difference between the two above approaches is almost a matter of detail. Avrami relates the changes in dX and dX' by heuristically assuming that, for a strictly uniform distribution of crystalline material, the constrained growth, dX, is a fraction $(1 - X)$ of the unconstrained one, dX'. On the other hand, Evans [4] provides a more detailed and clear description of the system, by recognizing that the arrivals of crystalline growth fronts at any point within the melt are *Poisson events* [16], characterized by an average number of occurrences (from time 0 to t) $\mu(t) = X'(t) = Kt^n$, from which he obtains $1 - X(t) =$ Probability of Zero Arrivals $= \mu^0 \exp(-\mu)/0! = \exp(-\mu)$ and, finally, Avrami's equation,

$$X = 1 - \exp(-Kt^n) . \tag{1}$$

It may be shown from basic growth geometry arguments, and as is well known [14], that K is proportional to the n^{th} or the $(n-1)^{\text{th}}$ power of the linear growth rate, G, for instantaneous or sporadic nucleation, respectively, as well as to the number of instantaneous nuclei or to the rate of nucleation, respectively.

In the ensuing discussion, the explicit and implicit assumptions made in the treatments will be considered in reasonable detail, though not fully [10]. To close this section, however, we think it appropriate to comment on the occasionally raised doubt about the validity of the impingement correction method always used – expressed basically by $dX = (1 - X)dX'$ – in cases other than spheres and parallel discs or needles. First, it should be clearly stated here that we are definitely dealing with spherulitic crystallization (overall spherical geometry), at least in the case of polymers, and so this problem may, for the moment, be considered somewhat lateral to the main theme of the work. Nevertheless, bearing in mind that the equality $dX = (1 - X)dX'$ requires that a strictly *uniform distribution of crystallized material* is assumed *at all times* (no matter how unlikely, or literally untrue that may appear), and that the crystallization is really *tridimensional* (i.e., even needles or discs have a finite, non-zero, thickness and may grow with their symmetry axes/planes having random, uniformly distributed locations and orientations), we may reasonably accept that

the only really significant limitation to the above equality is the eventual (or likely) non-uniform distribution of the crystallized phase, i.e., the breakdown of the original basic assumption itself.

2.2. Discussion of Avrami/Evans model

Wunderlich [5] lists and discusses some of the most obvious assumptions and limitations of the above general model, as applied to polymer crystallization. His comments do not need to be repeated here.

The most striking observation that almost invariably is made when this model is used to predict actual experimental polymer crystallization data (crystallized mass fractions, $X(t)$), as obtained by dilatometry, DTA/DSC or even other techniques, is that low values of the exponent n (Eq. (1)) are obtained, often of the order of 2. This has occurred and been widely published, in the past [17, 18], as well as recently [19, 20], despite the known but apparently ignored fact that such low exponents are not physically justifiable for reportedly spherulitic polymer crystallization. For pure materials, crystallizing as spheres, in the absence of strong diffusion effects, the n values should always lie between 3 and 4, depending on the type and rate of nucleation, and no model whatsoever may physically question that fact. It will be shown later in this report that this inconsistency disappears when alternative more accurate models are adopted, even when they are built upon the same two physical parameters of the Avrami/Evans model – K and n. The importance of a correct zero time setting in the experimental measurements will also be highlighted.

For this type of discussion, Evans approach has the distinct advantage of associating a definite and well known probabilistic model (*Poisson's distribution*) to the phenomena under analysis, which, as previously stated, are the arrivals of solid growth fronts to arbitrary points within the melt. In a way, one just has to fully discuss the nature and the assumption of such probability distribution to adequately assess it applicability and possible limitations. First, the conditions that define and validate Poisson's distribution [16] should be clearly stated, in the context of polymer crystallization:

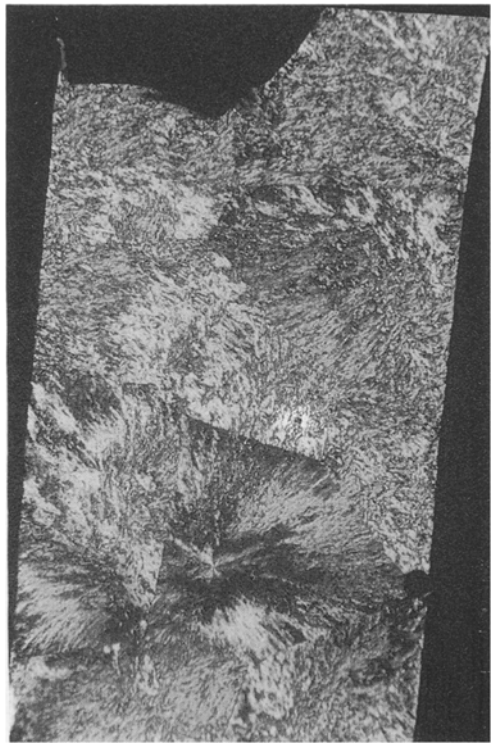

Plate 1: Polarized Optical Microphotograph of a Thin (0.7 mm) Section of a POM DSC Sample, after Crystallization at 157.0 °C

1) *infinite population* – i.e., the number of crystalline nuclei would have to be infinitely large (hardly true for some thin injection-molded parts and, in particular, DTA or DSC samples – see Plate 1).
2) *infinitely low unit probability* in terms of each contributing nuclei – i.e., $p = X'/(\text{No. of Nuclei}) \rightarrow 0$, which, with $X' = Kt^n$, $K \propto$ (No. of Nuclei) and $n \geq 1$, could only possibly hold at very short times, literally, when $X \rightarrow 0$;
3) *independent events* – i.e., the growth front arrivals would have to be independent of previous arrivals, which can only be approximated at infinitely low extents of crystallization – $X \rightarrow 0$ – exactly because crystal growth fronts do interfere with, and stop, each other at moderate and long times (by contrast, water waves in a pond [4] do not!).

Assumptions (1) and (2) are the result of Poisson's distribution being exactly such a limiting case of the *binomial distribution* ($N \rightarrow \infty$ and

$p \to 0$); its application to polymer crystallization has also been worked out, and compared with experiments [10, 21], and will be the subject of future reports. But, further, as (Np) is the average of the distribution, μ, and this must be *finite*, one immediately sees that making $\mu = X' = Kt^n$, as in Avrami/Evans model, does not fulfill that condition, especially at long times.

As a matter of fact, all amounts to μ being significantly overestimated at long times and, as $1 - X(t) = P(0) = e^{-\mu}$, the uncrystallized mass fraction is underestimated and, as a result, $X(t)$ may be grossly overestimated, as almost invariably found when comparing $X(t)$ predictions with measured data. The effect of then attempting to fit Avrami/Evans model to the data can be no other than the artificial decrease of the predicted X' values, expecially for long times, thus yielding too low values of n [17–20]; this is also illustrated in the results section of this paper.

2.3. Tobin's model – a quick review

Tobin's own derivation basis [6–8] may be very briefly outlined as follows:

a) individual grown spherulites are ideally sampled out, at time t;
b) their missing portions (due to impingement with other spherulites) are reconstituted;
c) each reconstituted drawn spherulite is then randomly thrown back to the original system.

The fraction of each reconstituted spherulite that will exactly fit the geometry it has been drawn from, without superposition with other spherulites, will on average be $[1 - X(t)]$ of its free growth mass. Therefore, the overall crystallized mass fraction should then be $X(t) = [1 - X(t)]X'(t)$ i.e., if $X' = Kt^n$ (exact for instantaneous nucleation, but only approximate for sporadic nucleation), *Tobin's equation* is obtained,

$$X(t)/[1 - X(t)] = Kt^n \quad \text{or} \quad X(t) = Kt^n/[1 + Kt^n] \,. \tag{2}$$

Under the same usual assumption of strictly uniform distribution of crystallized material, and at least for reasonably low values of $X(t)$, there is nothing wrong with above argument, no matter how strange (or too simple) it may seem. However, as X approaches 1, the uniformity assumption (from the standpoint of the drawn spherulite) completely breaks down, and one may anticipate that $X(t)$ may now be underestimated.

This somewhat unusual derivation did no catch attention, and apparently this resulted in a significant neglect of Tobin's papers [6–8], which otherwise notoriously provide much clear and valuable reading material. The very accurate treatment of the homogeneous thermal nucelation and of the phantom nuclei problem are good examples, leading to the expression

$$\frac{X(t)}{1 - X(t)} = nK \int_0^t (t - \tau)^{n-1}[1 - X(\tau)]\, d\tau \,, \tag{2a}$$

instead of Eq. (2).

It is strange that the literature still continues to overlook or mishandle this problem. Numerous authors appear to contend that the probability for a point not to be reached by any spherulites, $P(0) = 1 - X(t)$, is the same whether their appearance and growth are unconstrained or not, since a phantom entity cannot grow outside a real entity. Alas, even though such statements are strictly and literally true (only because phantom nuclei do *not* exist), when the average number of growth front arrivals to an arbitrary point, $\mu(t) = Kt^n$, is *calculated* with all phantom nuclei included in K, the only possible result definitely is, again, an overestimated μ and, of course, also an overestimated $X(t)$! This would equally apply whether one used Avrami/Evans equation (Eq. (1)) or the simplified Tobin's equation (Eq. (2)).

2.4. Tobin's model – a new derivation

The preceding discussion already suggests that at least the calculation of the Poisson's distribution average, μ, needs correction. As a matter of fact, the applicability of such probability distribution itself may indeed be questioned [10, 21], except as a limiting case ($N \to \infty$ and $p \to 0$), but this will not be the procedure adopted here. Instead, we will now reformulate the problem, taking only into account that the events concerned – solid growth front arrivals at arbitrary points within the melt – cannot be considered independent (see assumption 3 in section 2.2).

As is well known from elementary probability theory, when non-independent events determine and define the behavior of a system, *conditional probabilities* – generally denoted by $\boldsymbol{P}(\cdots|\cdots)$ – must be involved and duly taken into account in the formulation. So, let us denote the probability of zero arrivals at a given point up to time t by $\boldsymbol{P}(0, t)$ and the corresponding probability of one arrival by $\boldsymbol{P}(1, t)$. One may then write:

i) *Zero Events* (no phase change)

$$\boldsymbol{P}(0, t + dt) = \boldsymbol{P}(0, t) \cdot \boldsymbol{P}(0, dt|0, t)$$
$$= \boldsymbol{P}(0, t) \cdot [1 - \boldsymbol{P}(1, dt|0, t)] ,$$

or $-d\boldsymbol{P}(0, t)/\mathrm{P}(0, t) = \boldsymbol{P}(1, dt|0, t)$, i.e.,

$$\boldsymbol{P}(0, t) = \exp\left(- \int_0^t \lambda(t) dt \right) , \tag{3}$$

with

$$\lambda(t) = \boldsymbol{P}(1, dt|0, t)/dt = d\boldsymbol{P}(1, t|0, t)/dt. \tag{3a}$$

ii) *One Event* (local phase change)

$$\boldsymbol{P}(1, t + dt) = \boldsymbol{P}(0, t) \cdot \boldsymbol{P}(1, dt|0, t)$$
$$+ \boldsymbol{P}(1, t) \cdot \boldsymbol{P}(0, dt|1, t) ,$$

where $\boldsymbol{P}(0, dt|1, t) = 1$ (for single-mehanism crystallization processes, the phase change can only occur *once*) or, as $\boldsymbol{P}(0, t) = 1 - \boldsymbol{P}(1, t)$,

$$\boldsymbol{P}(1, t + dt) = [1 - \boldsymbol{P}(1, t)] \cdot \boldsymbol{P}(1, dt|0, t) + \boldsymbol{P}(1, t)$$
$$= \boldsymbol{P}(1, dt|0, t) + \boldsymbol{P}(1, t)$$
$$\cdot [1 - \boldsymbol{P}(1, dt|0, t)] ,$$

and $d\boldsymbol{P}(1, t)/[1 - \boldsymbol{P}(1, t)] = \boldsymbol{P}(1, dt|0, t) = \lambda(t)dt$, i.e.,

$$\boldsymbol{P}(1, t) = 1 - \exp\left(- \int_0^t \lambda(t) dt \right) . \tag{4}$$

Therefore, the main question is to correctly estimate $\lambda(t)$, defined by Eq. (3a), which involves a probability *conditioned by the previous non-occurrence of any phase change.* If the assumption of a uniform distribution of crystallized material is again made, the above conditional probability should be a fraction $(1 - X)$ of the corresponding unconditional, *fictitious* (free growth), probability, i.e., $\lambda(t)dt = (1 - X)dX'$, and Eq. (4) then yields

$$X(t) = 1 - \exp\left[- \int_0^t (1 - X) \frac{dX'}{dt} dt \right] , \tag{4a}$$

which, by differentiation, may be shown to exactly yield $dX = (1 - X)^2 dX'$ and, finally, Tobin's equation (Eq. (2)).

One may better understand the preceding paragraph if one realizes that the conditional probability $\boldsymbol{P}(1, dt|0, t)$ is the *fictitious*, free growth, *joint probability* of the occurrence of 0 events up to time t *and* 1 event during the additional time increment dt, i.e. $\boldsymbol{P}'(1, dt; 0, t)$, where this (now a joint probability of fictitiously independent events) must be given by the product of the corresponding fictitious probabilities, i.e., $\boldsymbol{P}(1, dt|0, t) = \boldsymbol{P}'(1, dt) \cdot \boldsymbol{P}'(0, t) = (1 - X)dX'$, as obtained above. In the previous equality, $\boldsymbol{P}'(0, t)$ cannot differ from $\boldsymbol{P}(0, t)$, because no fictitious growth occurs outside the actually growing entities, and so $\boldsymbol{P}'(0, t) = \boldsymbol{P}(0, t) = 1 - X$.

It may therefore be concluded, from this new derivation, that Tobin's model is a fairly accurate representation of single-mechanism crystallization processes from a melt, subject to only two main conditions – 1) infinite number of nuclei and 2) strictly uniform distribution of crystallized material at all times.

It may be easily checked that now both the probability per nuclei, and the overall probability density per unit time, $\lambda(t)$, are always finite. Actually, as one would expect, $\lambda(t)$ is 0 at $t = 0$ and when $t \to \infty$, with a maximum at an intermediate time. By contrast, dX'/dt always increases with t towards ∞, which is physically unacceptable.

3. Modeling of complex crystallization processes

3.1. Hillier's model

Hillier, following attempts by other authors referred to in his paper [11], considered that any differential mass of crystallizing material is first converted by an α-, Avrami-like, mechanism, and then gradually "re-crystallizes" according to a second β-, also Avrami-like, mechanism. In this way, both mechanisms are simultaneously operating within any finite sample of the material, but strictly follow each other from the standpoint of any differential mass of the sample.

Denoting by $\chi_{\alpha m}$ the maximum true crystallinity locally obtained by the α-mechanism and by $\chi_{\beta m}$ the maximum additional crystallinity gained

by the material in the β-process, Hillier [11] calculated the overall crystallinity at time t, $\chi(t)$, by

$$\chi(t) = \chi_\alpha(t) + \int_{t-\tau=0}^{t-\tau=t} \frac{\chi_\alpha(\tau)}{\chi_{\alpha m}} d\chi_\beta(t-\tau) , \quad (5)$$

where $\chi_\alpha(t)$ and $\chi_\beta(t-\tau)$ both obey Avrami's model, i.e., $\chi_\alpha(t) = \chi_{\alpha m}\,[1 - \exp(-K_\alpha \cdot t^{n\alpha})]$ and

$$\chi_\beta(t-\tau) = \chi_{\beta m}\{1 - \exp[-K_\beta \cdot (t-\tau)^{n\beta}]\} .$$

Dividing both sides of Eq. (5) by $(\chi_{\alpha m} + \chi_{\beta m})$ – the maximum final crystallinity – one then easily obtains for the overall transformed mass fraction, $X(t)$,

$$X(t) = X_\alpha(t) + X_{\beta m} K_\beta n_\beta \int_0^t (1 - e^{-K_\alpha \tau^{n_\alpha}}) \times (t-\tau)^{n_\beta - 1} e^{-K_\beta (t-\tau)^{n_\beta}} d\tau , \quad (6)$$

with $X_\alpha(t) = X_{\alpha m} \cdot [1 - \exp(-K_\alpha \cdot t^{n\alpha})]$, and where $X_{\alpha m} = \chi_{\alpha m}/(\chi_{\alpha m} + \chi_{\beta m})$ and $X_{\beta m} = 1 - X_{\alpha m}$ denote the maximum material fractions transformed by each of the mechanisms.

3.2. *Modified Hillier's model*

Actual fittings of Hillier's model to experimental data are relatively rare [9, 11, 22], but very commonly yield values $\leqq 1$ for n_β. Actually, Hillier himself [11] only considered $n_\beta = 1$, with $n_\alpha = 3$ or 4.

As a consequence, the evaluation of the integral in Eq. (6) may be significantly affected by large inaccuracies near $\tau = t$ (singularity), when n_β comes below 1, which inevitably interfere with the course and the results of any parameter optimization procedure. This problem may, however, be entirely avoided if Hillier's analysis is modified as follows: any fraction of material that undergoes the α-process, $dX_\alpha(\tau)$, should then follow the β-mechanism from τ to t, such that its overall crystallinity changes according to

$$\chi(t) = \chi_\alpha(t) + \int_0^t \chi_\beta(t-\tau) dX_\alpha(\tau) , \quad (7)$$

where $\chi_\alpha(t)$ and $\chi_\beta(t-\tau)$ are obtained from whatever models one chooses to describe those mechanisms.

The really new step is the selection of Tobin's model on the grounds of its better physical basis and higher accuracy, i.e. $\chi_\alpha(t) = \chi_{\alpha m} K_\alpha \cdot t^{n_\alpha}/(1 + K_\alpha \cdot t^{n_\alpha})$ and $\chi_\beta(t-\tau) = \chi_{\beta m} K_\beta \cdot (t-\tau)^{n_\beta}/[1 + K_\beta \cdot (t-\tau)^{n_\beta}]$. It may then be shown that Eq. (7), after dividing both sides by $(\chi_{\alpha m} + \chi_{\beta m})$, reduces to

$$X(t) = X_\alpha(t) + X_{\beta m} K_\alpha K_\beta n_\alpha \times \int_0^t \frac{\tau^{n_\alpha - 1}(t-\tau)^{n_\beta}}{(1 + K_\alpha \tau^{n_\alpha})^2 [1 + K_\beta (t-\tau)^{n_\beta}]} d\tau , \quad (8)$$

with $X_\alpha(t) = K_\alpha \cdot t^{n_\alpha}/(1 + K_\alpha \cdot t^{n_\alpha})$.

In this form, no singularity is obtained for any value of n_β, and the ensuing parameter optimization procedures become much safer and able to yield meaningful results. The maximum number of physical parameters in Eq. (8) will thus be 5 but, for polymers like POM, it will be shown later in this report that the parameters may be only 4, i.e., $X_{\alpha m}$, K_α, K_β and $n_\alpha = n_\beta$, which is by no means excessive if one can achieve an accurate and physically consistent description of really complex crystallization processes.

Of course, the possibility of other types of secondary mechanism cannot be ruled out, particularly the thickening of previously grown lamellae. As may be shown in future reports, the formalism presented here may then also be generalized.

4. Experimental

4.1. *Materials*

The poly(oxymethylene) – POM – used in the experiments of this study was a well characterized [23–25] commercial grade – DELRIN 150 ($T_m^0 = 198.3\,^\circ C$, $T_g = -82$ to $-74\,^\circ C$, N-average mol. w. $\approx 70\,000$ g/mole). The poly(ether-ether-ketone) – PEEK – used was of grade 450 G, kindly supplied by ICI.

4.2. *Differential scanning calorimetry (DSC)*

The isothermal DSC experiments were carried out on a Perkin-Elmer DSC7, using a controlled temperature jump procedure [9], from above the melting point to the crystallization temperature. These experiments were preceded by a thorough calibration of the instrument, using two standards, at a scanning rate of $0.2\,^\circ C$/min. The instrument was fitted with an external block temperature control system set at $-90\,^\circ C$. For

each isothermal scan, blank runs were also performed with the same sample, at a temperature at which no phase change had occurred (above the melting point), to fully account for and eliminate the initial transient heat capacity signal – proportional to $C_p \cdot (dT/dt)$ – that is obtained in every DSC temperature jump experiment. Consistent sample heat treatments were used prior to each run which, combined with the high precision and accuracy of the calorimeter, ensured exactly reproducible DSC traces at each crystallization temperature, to accurately characterize the sample's behavior. The DSC data were obtained to within less than 5 μW and 10^{-3} min.

Care was also taken to measure the crystallization time from the very beginning of the isothermal period, under temperature control, and *not* from the onset of the exothermal crystallization peak. This procedure, which is very commonly used [22, 26], is physically incorrect (whatever chemical or physical change is studied), not only formally, but also because it neglects the induction period that so commonly exists in nucleation-controlled phase changes. The influence of this procedure on the measured data and their interpretation will be dealt with in the results section.

4.3. Optical microscopy (OM)

The optical microscopy crystallization studies (spherulite radial growth rate measurements) and structure observations on POM were carried out on a Mettler FP82 hot stage, under a polarizing microscope fitted with a 530 nm retardation plate. Before each of the isothermal crystallization experiments, the material was melted and heated up to 200 °C to erase its thermal history; no thermal degradation was ever detected (as assessed by DSC). Then, the temperature was quickly lowered to the chosen crystallization temperature, and the spherulites were photographed, at intervals, to measure their radii as functions of time. A few non-isothermal measurements were also carried out in a similar way, by cooling the material in the hot stage from 200 °C at constant cooling rates of 1 °C/min and 5 °C/min [25]. All photographs had exposure times shorter than 1 s.

After some of the isothermal scans, DSC samples of POM were sliced on a microtome and observed on the same polarizing microscope, to ascertain the type of structures obtained.

5. Results and discussion

Although this work concentrates on the isothermal crystallization of POM and PEEK, we also felt it necessary to extend the methods and basic models proposed here to a wider range of materials. Many other polymers have already been and are being studied (PET, several polyethylenes, PP, POE, etc.), as well as some metals – the widely used DSC standards In and Pb [10, 21], and so a short preliminary presentation of a sample of such data seems relevant, awaiting more detailed future reports.

Two typical isothermal DSC scans are shown in Fig. 1 for a pure metal (Pb) and a medium density polyethylene (MDPE), to illustrate the temperature jump procedure and the time measurement method used. They clearly show that the influence of the time origin setting may be very significant, as, for example, in the case of Pb: successive crystallizations of the same sample, exactly at the same temperature, gave exactly reproducible peaks and consistently showed an apparent induction time of almost 0.8 min. The effect in the case of POM crystallizing at 157 °C is also illustrated in Fig. 2 (Avrami-type plot), which clearly shows that an incorrect zero time setting (+ symbols) may wrongly lead to the conclusion that Avrami's model may in this case exactly fit the data with $n = 2$, while in fact that is not so (○ symbols and solid, Tobin-predicted, curve with $n \approx 4$). Polarized light microscopy observations of this material at the same temperature clearly confirm that the crystallization is spherulitic with sporadic nucleation, and so n should be of the order of 4 (see Plate 2). At lower temperatures (see also Fig. 2), the influence of the zero time setting may be less significant.

The suitability and accuracy of Tobin's two-parameter model (Eq. (2)) to describe single-mechanism crystallization processes of a wide range of materials (other than POM and PEEK) may be illustrated by Figs. 3 and 4 (In/Pb) and 5 (MDPE). For the two metals, while the Avrami's type of plot ($\log_{10}[-\ln(1-X)]$ vs. $\log_{10} t$) yield lines of pronounced curvature, Tobin's plots ($\log_{10}[X/(1-X)]$ vs. $\log_{10} t$) are exactly linear from X below 0.09 to X higher than 0.999 (marked in the diagrams) and, for MDPE, we again see that Tobin's model is far superior to Avrami's, yielding quite accurate fits to the data

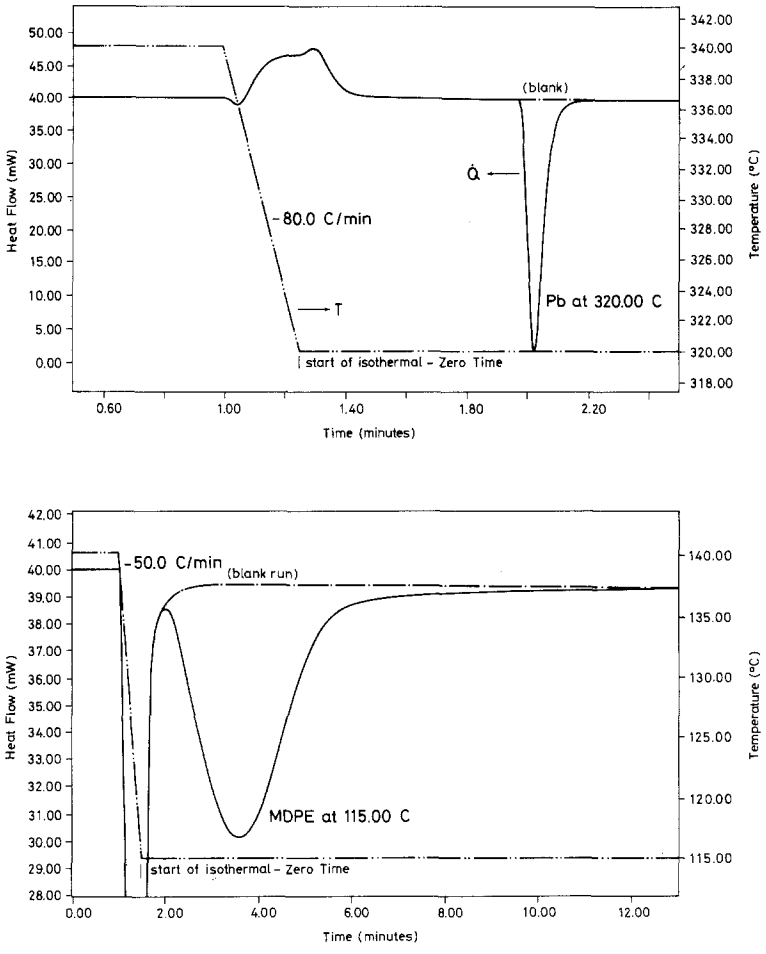

Fig. 1. DSC isothermal crystallization traces for lead (320 °C) and a medium density polyethylene (115 °C)

with $n = 4$, which is consistent with a non-instantaneous nucleation of spherulites [21].

Data for a well characterized poly(oxyethylene), PE from Aldrich (18, 947-2) have been recently obtained, which are also accurately described by Tobin's model [27].

5.1. *Poly(oxymethylene) – POM*

Figure 6 shows four experimental Avrami-type isothermals for POM, together with the theoretical predictions by Avrami's (Eq. (1)), Tobin's (Eq. (2)) and the original Hiller's (Eq. (6)) models. Tobin's two-parameter model predictions (solid lines) undoubtedly are the most accurate, even clearly surpassing Hillier's original four-parameter ($n_\beta = 1$) model predictions (broken lines); as expected, Hillier's predictions only significantly differ from Avrami's (–·– straight lines) for very long times. When n_β was also allowed to vary (five parameters), Hillier's model predictions did not show any significant improvement.

As for the parameter values, Table 1 shows the n values obtained by the Avrami's and Tobin's models for nine different isothermals; in general, while $2 < n_{\text{Avrami}} < 3$, one obtains $3 < n_{\text{Tobin}} < 4$, which indicate that only Tobin's model n values are entirely consistent with a well defined spherulitic crystallization (see Plates 1 and 2). Further, the values of $K^{1/n}$ obtained may be shown (Fig. 7) to practically coincide (+ and ○ symbols) with the experimental (DSC-measured) reciprocal crystallization half-times, $(1/t_{0.5})$, as exactly expected from theory (Eq. (2)), and their variation with the crystallization temperature also follows very closely that of the spherulite linear growth rates, G, measured by optical microscopy [25]. In the abcissa of Fig. 7, ΔT is the degree of supercooling, and f is the usual correction factor that takes into account the

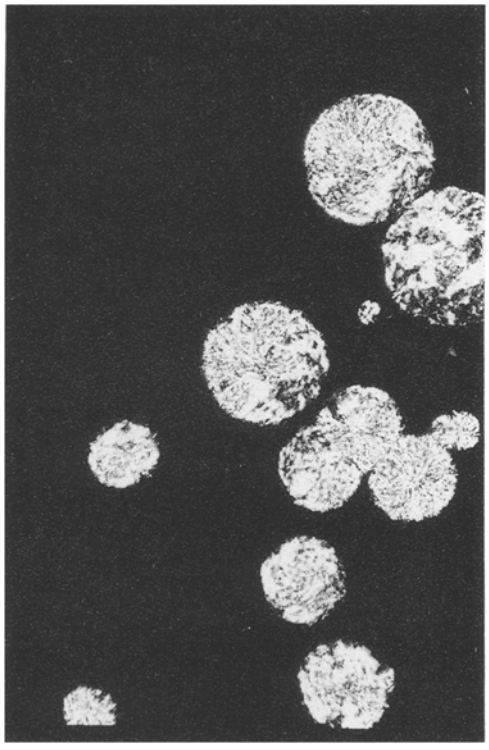

Plate 2: Polarized Optical Microphotograph of a Thin Film of POM Crystallizing on a Hot State at 157.0 °C

decrease of the heat of fusion with the crystallization temperature, i.e., $f = 2T/(T_m^0 + T)$.

The experimental isothermal crystallization data of various polymers, however, often show that a secondary process may possibly be operating at long times [9, 11]; so, it is also important to test the usefulness and accuracy of the models presented in sections 3.1 and, especially, 3.2. A set of POM isothermals is plotted in Fig. 8, together with the theoretical predictions by Tobin's (Eq. (2)) and the modified Hillier's (Eq. (8)) models; as initial five-parameter optimization attempts yielded n_β values very similar to those of n_α, the calculations were then continued using only four adjustable parameters ($X_{\alpha m}$, K_α, K_β and $n_\alpha = n_\beta$), with the excellent results shown. The predictions are now, as expected, better than Tobin's two-parameter, single-mechanism model predictions, and (as already stated) very much better than those of the original Hillier's model (Eq. (6)); the relative merits of the different models may also be easily assessed from the corresponding sum of least squares plotted in Fig. 9. It is nevertheless interesting to note that, for the lowest temperatures (149 °, 150 °, and 151 °C), the two-parameter, single-mechanism Tobin's model is already sufficiently accurate (same sum of least squares as the modified Hillier's model).

The ability to predict physically meaningful values for the whole set of parameters – K_α, K_β, n_α, n_β and $X_{\alpha m}$ – is, of course, important to validate the use of the modified Hillier's model. Their predicted optimum values are plotted in Figs. 7, 10 and 11, and are discussed below.

In some previous works where the original Hillier's model was used [9, 11, 22], only the K_α (or K_α^{1/n_α}) values could easily be related to the crystalline linear growth rate, G. By contrast, in this new,

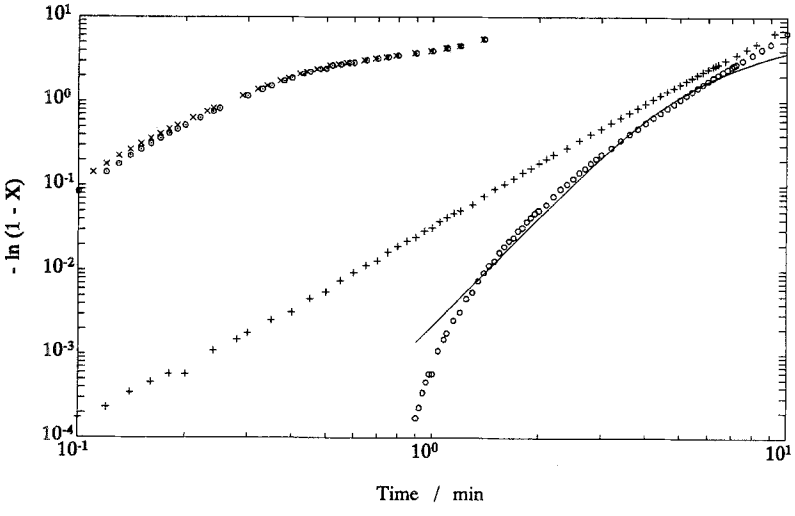

Fig. 2. Effect of the zero time setting on the interpretation of DSC isothermal crystallization data (○, + POM at 157 °C; —two-parameter, single Tobin's model with $n = 4$; ○, × POM at 149 °C)

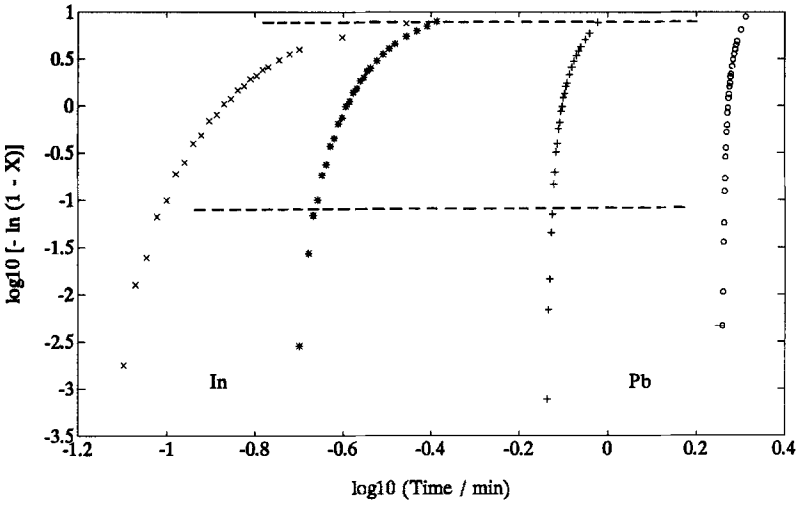

Fig. 3. Avrami-type plot of indium (* 152 °C; × 150 °C) and lead (○ 321 °C; + 320 °C) crystallization data

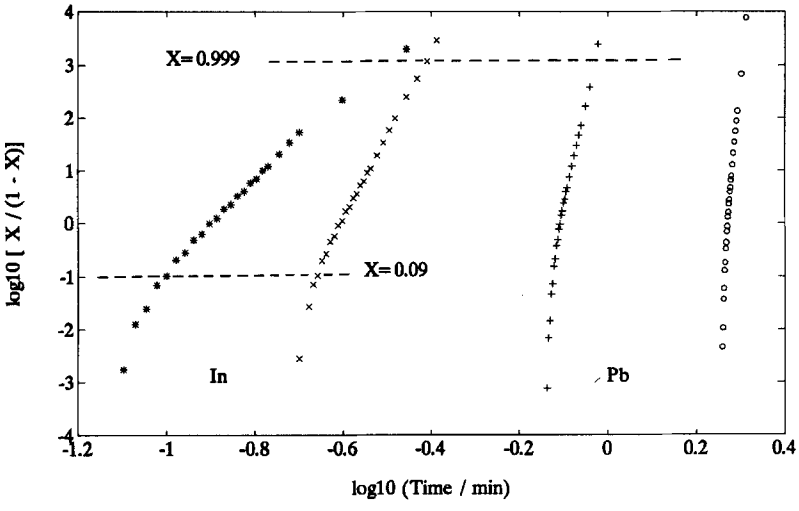

Fig. 4. Tobin-type plot of indium (* 152 °C; × 150 °C) and lead (○ 321 °C; + 320 °C) crystallization data

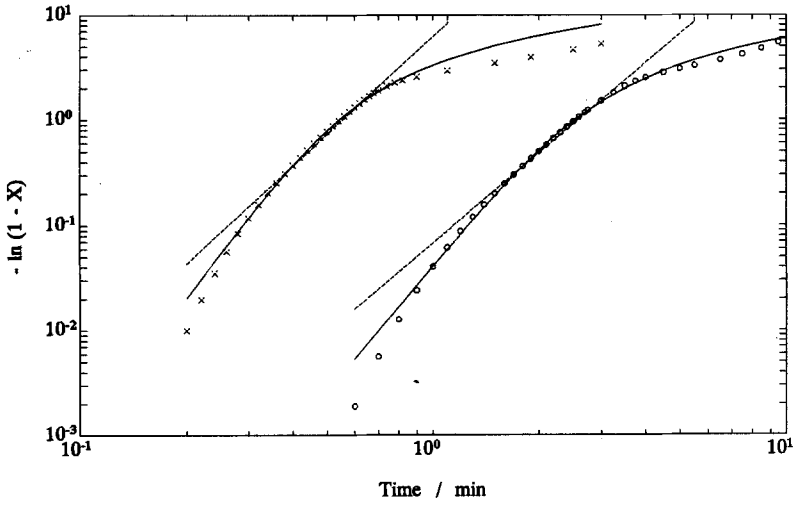

Fig. 5. Isothermal cyrstallization of MDPE (○ 115 °C; × 110 °C; --- Avrami's model; — Tobin's model)

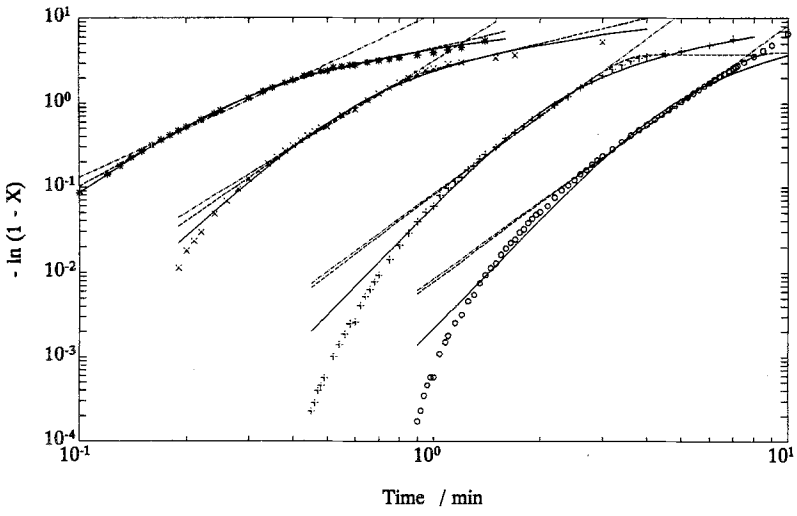

Fig. 6. Isothermal crystallization of POM (○ 150 °C; + 155 °C; × 152 °C; * 149 °C; –·– two-parameter, single Avrami's model; – – – four-parameter, Avrami-based Hillier's original model with $n_\beta = 1$; — two-parameter, single Tobin's model)

Table 1. Isothermal Crystallization of POM. Values of the Avrami and Tobin exponents obtained by the application of Equations (1) and (2), respectively

T (°C)	n_{Avrami}	n_{Tobin}
149	1.93	2.96
150	2.20	3.30
151	2.44	3.51
152	2.58	3.69
153	2.79	3.95
154	3.00	4.24
155	3.04	4.27
156	3.07	4.34
157	2.99	4.27

Tobin-based, modified form (Eq. (8)), one may physically interpret both K_α and K_β; in fact, as may be seen in Fig. 7, both K_α^{1/n_α} and K_β^{1/n_β} show a dependence on temperature similar to that of $1/t_{0.5}$, the main difference being that, for POM, the β-process is faster than the α-process.

The n values ($n_\alpha = n_\beta$) obtained vary with the crystallization temperature in the regular manner shown in Fig. 10, from a low temperature (< 149 °C) limit of 3 to a high temperature ($\geqq 156$ °C) one of about 5. This, again, is entirely consistent with a spherulitic crystallization (Plates 1 and 2), with the initial formation of more open, sheaf-like structures at the higher temperatures (Plate 2), for which dimensionalities in excess of 4 may in fact be expected [5, 9, 28]. The fact that the model naturally yields the same values for n_α and n_β indicates that, generally speaking, only an internal fast reorganization of the spherulitic material, within the same overall geometry, may be involved in the β-process.

Both at high temperatures (slow nucleation of relatively open structures, $n > 4$) and at low temperatures (faster nucleation of well defined spherulites, $n = 3$), the predicted behavior of POM is consistent with the formation of a hierarchy of lamellae within the same overall geometry – primary, α-lamellae, followed by thinner, more rapidly grown β-lamellae, possibly by surface nucleation of lower molecular weight material on the previously formed α-lamellae. The problem surely requires further study, but optical and electron microscopy observations by Pelzbauer and Galeski [23] on the same material, and by Bassett et al. on polyethylene [29] and generally on polyolefins [30] appear to confirm this type of structures and behavior. What Basset and coworkers essentially found was that the overall spherulitic geometry is defined by the dominant α-lamella, which grow by splaying and branching, and the β-process then follows, leading to a seemingly more fibrous texture.

The variation of the predicted $X_{\alpha m}$ and $X_{\beta m}$ (maximum material fractions transformed by each of the mechanisms) is also very regular, as shown in Fig. 11. The way they vary with the crystallization temperature must be related to the relative kinetics of the α (slowest) and β (fastest) processes, as well as to the geometry of the structures. It may in fact be expected that, in the case of the not fully grown, relatively open spherulites

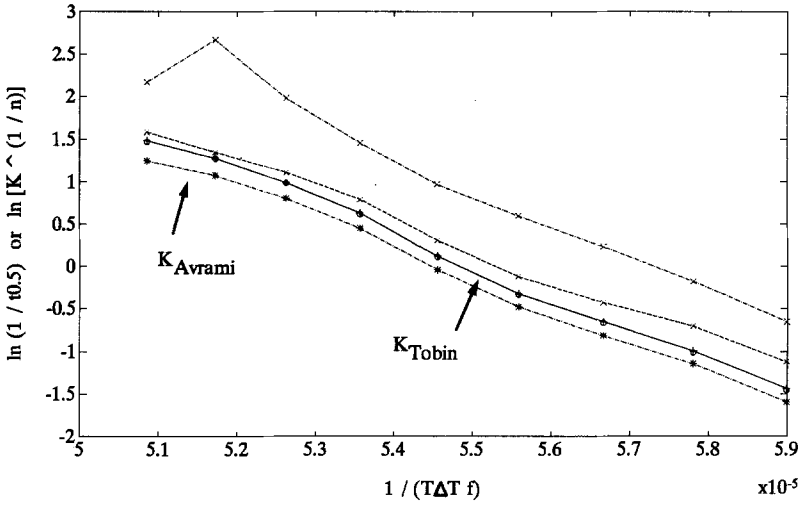

Fig. 7. Dependence on temperature of the experimental (DSC) reciprocal crystallization half-times ($1/t_{0.5}$) and of the various predicted $K^{1/n}$ for POM (○ $\exp^{al}$ $1/t_{0.5}$; ∗ two-parameter, single Avrami's model; + two-parameter, single Tobin's model: – – × – – predicted $K_{\alpha}^{1/n\alpha}$; – · × · – predicted $K_{\beta}^{1/n\beta}$)

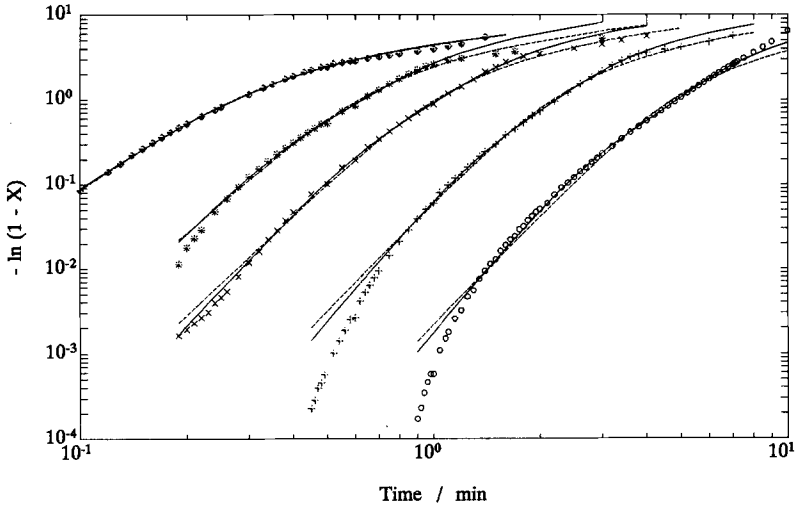

Fig. 8. Isothermal crystallization of POM (○ 157 °C; + 155 °C; × 153 °C; ∗ 152 °C; ○ 149°C; – – – two-parameter, single Tobin's model; — four-parameter, Tobin-based, Hillier's modified model)

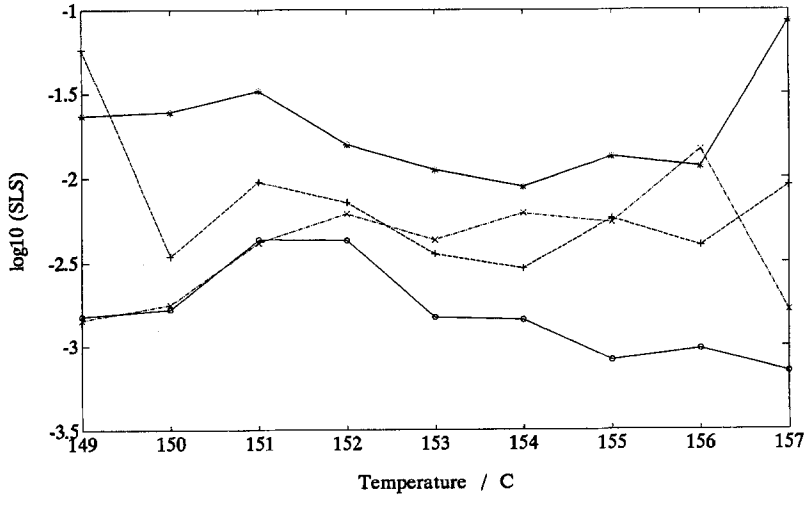

Fig. 9. Sum of least squares (SLS) comparison of different models for POM (∗ two-parameter, single Avrami's model; + four-parameter, Avrami-based, original Hiller's model; × two-parameter, single Tobin's model; ○ four-parameter, Tobin-based, modified Hillier's model)

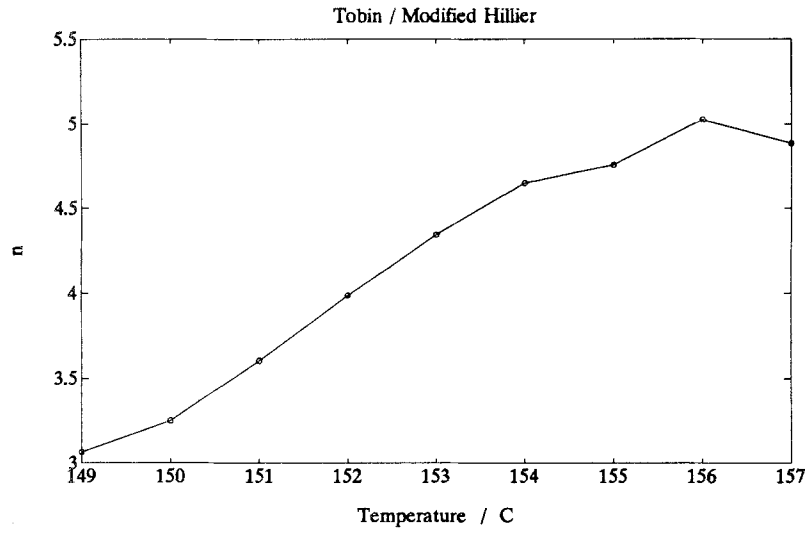

Fig. 10. Variation with temperature of the $n_\alpha = n_\beta$ values predicted for POM by the Tobin-based, modified Hillier's model

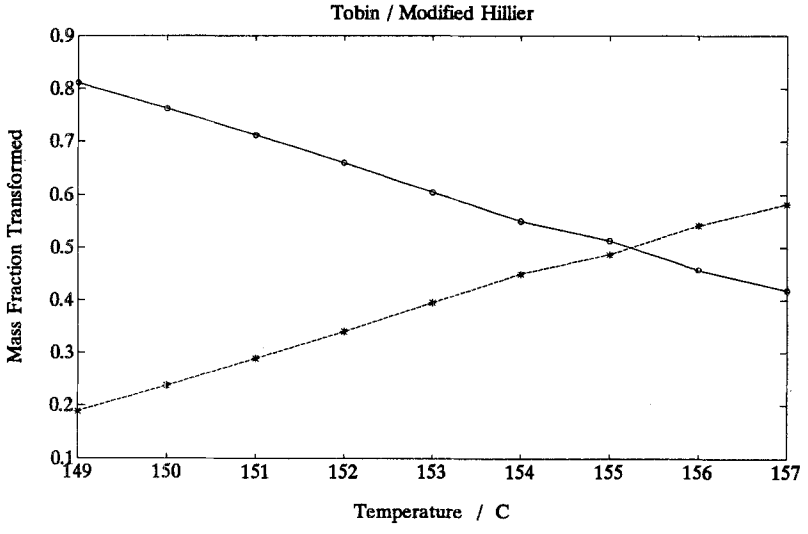

Fig. 11. Variation with temperature of the $X_{\alpha m}$ (○) and $X_{\beta m}$ (*) values predicted for POM by the Tobin-based, modified Hillier's model

formed at high temperatures, the faster β-mechanism should be responsible for higher extents of secondary crystallization ($X_{\beta m} > X_{\alpha m}$); at low temperatures, however, only a relatively smaller amount of material would be available for secondary crystallization within the much more compact spherulites formed, which explains the relatively lower $X_{\beta m}$ values ($X_{\beta m} < X_{\alpha m}$), despite the higher specific rate of the β-process.

Thus, for POM, the superiority of Tobin's (two-parameter) and Tobin's-based, modified Hillier's (four-parameter) models is hereby clearly demonstrated. The quality of the fits to the experimental data with so few parameters, and the meaningful values obtained for those parameters, clearly support the reasonableness and accuracy of the methods and models presented here. As already explained, however, these models may still need some adjustment to account for the possible presence of only a small number of nuclei. The problem will be dealt with in future publications, but first results [10] confirm that the effect may be significant only for long crystallization times.

5.2. *Poly(ether-ether-ketone) – PEEK*

In the case of PEEK, the need to consider a secondary crystallization process is clearly

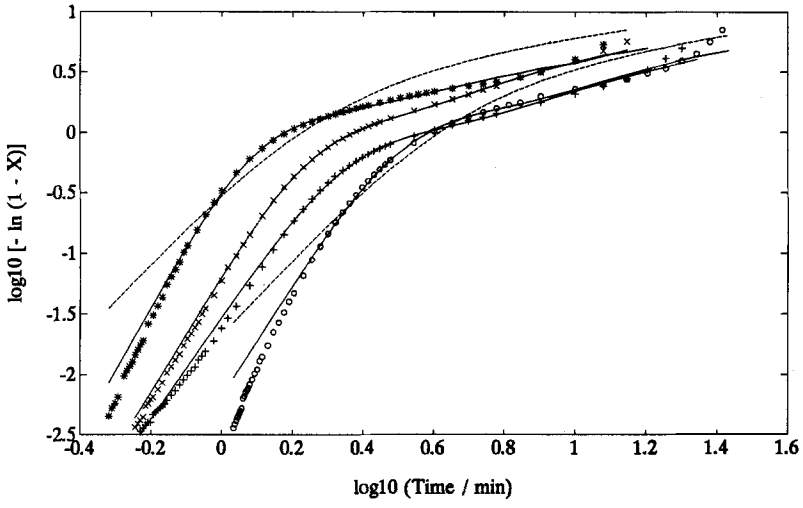

Fig. 12. Isothermal crystallization of PEEK (○ 315 °C; + 312 °C; × 310 °C; * 307 °C; --- two-parameter, single Tobin's model; — five-parameter, Tobin-based, modified Hillier's model)

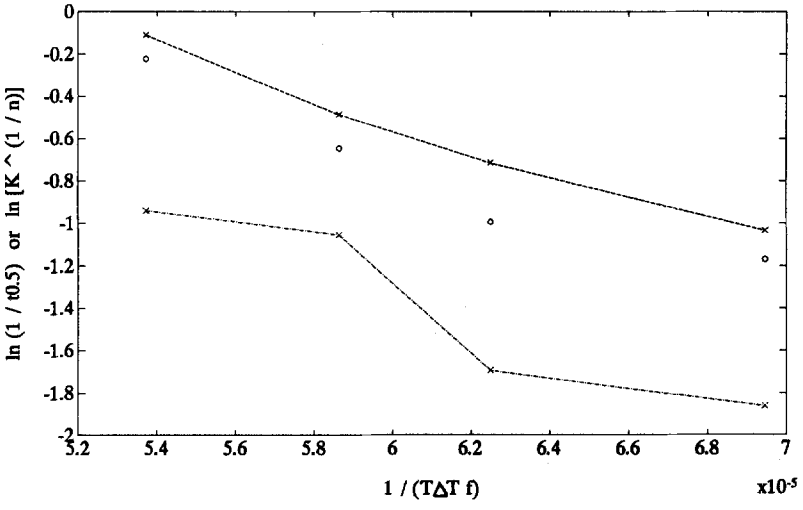

Fig. 13. Dependence on temperature of the $K_{\alpha}^{1/n\alpha}$ (--×--) and $K_{\beta}^{1/n\beta}$ (-·×·-) values predicted for PEEK by the Tobin-based, modified Hillier's model (○ exp^{al} $1/t_{0.5}$)

greater than with POM. As shown in Fig. 12, the fits by a single two-parameter Tobin's equation are much poorer than with other materials, although again it clearly surpasses the accuracy of the classical Avrami/Evans model; this earlier model would predict an exactly linear variation of $\log_{10}[-\ln(1-X)]$ with $\log_{10}(t)$, while Tobin's model at least succeeds in predicting the right type of curvature (broken lines for the isothermals at 307 °C and 315 °C).

When the secondary process is modeled, as proposed in this work, according to Eq. (8), very accurate predictions of the experimental behavior are achieved (solid lines); however, for this material, this required the use of different n_{α} and n_{β} values, i.e., five parameters. While n_{α} is predicted to lie between 4 and 5 (perhaps consistent with the formation of less perfect spherulites), the n_{β} values fall between 2 and 2.5, which is not so easy to explain. Optical microscopy observations of this material (using a high temperature hot-stage accessory) will be needed to adequately analyze the crystallization behavior of PEEK.

Nevertheless, the model predicts that with PEEK, by contrast with POM, the α-process is now the fastest, as shown in Fig. 13, and this seems to be confirmed by recent optical microscopy observations by Phillips [31] on other samples of PEEK. The predicted values of $X_{\alpha m}$, which range from 0.65 to 0.77 (Table 2), seem to be

Table 2. Isothermal crystallization of PEEK. Some parameter values obtained by application of Eq. (8)

T (°C)	$X_{\alpha m}$	n_α	n_β
307	0.75	5.28	1.88
310	0.72	4.87	2.38
312	0.65	4.28	2.23
315	0.78	4.60	2.50

consistent with the higher rate of the α-process. In Fig. 13, it may also be seen that the values of K_α^{1/n_α} show a dependence on temperature similar to that of $1/t_{0.5}$; the behavior of K_β^{1/n_β}, however, is less regular.

As already stated, careful microscopy observations are being planned to clarify the type of structures that are obtained with PEEK before this work may be considered complete. Also, the possibility of lamella thickening being the main contributor to the secondary process is also being analyzed. This could explain the less regular variation of K_β^{1/n_β} with $1/(T\Delta Tf)$.

6. Conclusions

1. Tobin's model, with only two parameters, provides a much more accurate description of single-mechanism crystallization processes than the earlier Avrami/Evans model, for a wide range of materials, such as pure metals and a variety of polymers. A new derivation of Tobin's model has been developed, which gives it a firm physical and mathematical basis.
2. More complex (multi-stage) crystallization processes of materials like POM may be accurately described by a modified version of Hillier's model, which incorporates a Tobin-like behavior of each of the contributing mechanisms. The model requires only four parameters.
3. Physically meaningful values have been obtained for the model parameters, as well as for their variations with temperature. The predicted values show a remarkable consistency with the microstructures and behavior observed for POM by the present and many other authors.
4. For materials like PEEK that show a more pronounced and complex secondary crystallization behavior, the same basic modeling strategy may be used, with only possible adjustments needed on the actual nature of the secondary process, e.g., formation of new lamellae vs. lamella thickening. With this material further work is still necessary.

Acknowledgements

We acknowledge the financial support obtained from *FLAD (Luso-American Foundation)*, *PEDIP (Portuguese Industrial Development Plan)*, and the *CIÊNCIA Programme. ICI (Imperial Chemical Industries)* is also thanked for kindly supplying PEEK.

References

1. Avrami JM (1939) J Chem Phys 7:1103
2. Avrami JM (1940) J Chem Phys 8:212
3. Avrami JM (1941) J Chem Phys 9:177
4. Evans UR (1945) Trans Faraday 41:365
5. Wunderlich B (1976) Macromolecular Physics Vol. 2 Crystal Nucleation, Growth, Annealing. Academic Press
6. Tobin MC (1974) J Polym Sci, Polym Phys Ed 12:399
7. Tobin MC (1976) J Polym Sci, Polym Phys Ed 14:2253
8. Tobin MC (1977) J Polym Sci, Polym Phys Ed 15:2269
9. Martins JA (1991) M.Sc. Dissertation, Universities of Minho and Lisboa, Portugal
10. Cruz-Pinto JJC (1992) 'Towards a General Model of Phase Changes - The Experimental, Physical and Mathematical Problems', Professorship Lecture, University of Minho (to be published)
11. Hillier IH (1965) J Polym Sci, Part A 3:3067
12. Velisaris CN, Seferis JC (1986) Polym Eng & Sci 26:1574
13. Cebe P (1988) Polym Eng & Sci 28:1192
14. Schultz JM (1974) Polymer Materials Science Ch. 9 – Crystallization Kinetics and Mechanism. Prentice-Hall
15. Sperling LH (1992) Introduction to Physical Polymer Science Ch. 6 – The Crystalline State. Wiley-Interscience
16. Meyer SL (1975) Data Analysis for Scientists and Engineers Ch. 24 – The Poisson Distribution. John Wiley & Sons Inc
17. Banks W, Sharples A (1963) Makromol Chem 59:283
18. Mandelkern L (1964) Crystallization of Polymers, p 237. McGraw-Hill
19. Kim SP, Kim SC (1991) Polym Eng & Sci 31:110
20. Menczel JD, Collins GL (1992) Polym Eng & Sci 32:1264
21. Cruz-Pinto JJC, Martins JA (1992) IUPAC Macro '92: 2-P175, Prague, Czechoslovakia
22. Kamal MR, Chu E (1983) Polym Eng & Sci 23:27
23. Pelzbauer Z, Galeski A (1972) J Polym Sci Polym Phys Ed 38:23
24. Hoffman JD (1983) Polymer 29:3
25. Martins JA, Cruz-Pinto JJC, Oliveira MJ (1993), J Thermal Anal 40:629
26. Seferis JC (1991) 23rd Europhys Conf Macromol Phys: Invited Lecture L34, Stockholm, Sweden
27. Cruz-Pinto JJC, Martins JA (1993) In Dosiere M (ed) Crystallization of Polymers. NATO ASI Series C (Mathematical and Physical Sciences) 405:257. Kluwer Acad Publs

28. Morgan LB (1954) Phil Trans Roy Chem Soc (London) 247:13
29. Bassett DC (1993) In Dosiere M (ed) Crystallization of Polymers. NATO ASI Series C (Mathematical and Physical Sciences) 405:107 (and references Therefrom). Kluwer Acad Publs
30. Bassett DC, Olley RH (1984) Polymer 25:935
31. Phillips PJ (1992) NATO ARW on Crystallization of Polymers (discussions on recent results), Mons, Belgium

Received February 23, 1993;
accepted March 4, 1993

Authors' address:

Prof. Dr. J. J. C. Cruz-Pinto
Department of Polymer Engineering
University of Minho
4719-Braga Codex
Portugal